Crack Growth Behavior of F82H Steel in the 288°C water

Yuzuru ITO[a], Masahiro SAITO[b], Katsunori ABE[b] and Eiichi WAKAI[a]

[a] *Japan Atomic Energy Agency, Ibaraki, Japan*

[b] *Hachinohe Institute of Technology, Aomori, Japan*

(Received: 17 September 2014 / Accepted: 19 January 2015)

Crack growth is a key mechanical property that must be considered in the design of fusion reactor materials to be tested at the high flux test module in the International Fusion Materials Irradiation Facility. In this study, crack growth behavior of F82H steel was investigated to determine its crack growth rate in water at 288°C. The crack growth tests were conducted for approximately 1000 h using specimens with dimensions similar to the standard dimensions. A typical intergranular fracture surface was obtained during crack propagation at room temperature in air. The precipitation of chromium carbide, $Cr_{23}C_6$, along the grain boundaries in F82H steel may influence the fracture behavior in cases such as fatigue crack propagation at room temperature in air. The crack growth rate at 30 MPa·$m^{1/2}$ was evaluated to be approximately 7×10^{-11} m/s

Keywords: IFMIF, F82H steel, Crack growth, Chromium carbide, High temperature water

1. Introduction

Structural and functional materials used in the fusion demonstration reactor (DEMO) will be exposed to neutrons with energies as high as approximately 14 MeV at approximately 3.5 MW/m^2 (5.0 MW/m^2 at the peak) and with a fluence greater than 10 MW·s/m^2 during the reactor's operation. Radiation damage of materials in a fusion reactor environment can be characterized by synergistic effects of displacement damage and nuclear transmutation products such as hydrogen and helium atoms [1-6]. These damages result in the degradation of mechanical properties. For fusion nuclear reactors to be safely operated, the detailed behavior of material degradation with respect to a 14 MeV neutron dose must be understood. The International Fusion Materials Irradiation Facility (IFMIF) generates high-energy deuterium–lithium neutrons for irradiation experiments of candidate fusion reactor materials; researchers are using this neutron source to construct a database from a series of tests of small-sized specimens for the fusion DEMO reactor's design and licensing [7]. The irradiation volume of the IFMIF is approximately 14 L, and the greatest displacement damage is greater than 20 dpa (displacement per atom)/year in a volume of 0.5 L. Approximately 1000 specimens need to be irradiated in the IFMIF high flux test module (HFTM) within a limited volume of approximately 0.5 L, as recommended by [8]. Therefore, small specimens must be used for this purpose; the development of a small specimen test technique or technology (SSTT) is therefore very important [9]. In the IFMIF/EVEDA (Engineering Validation and Engineering Design Activities) program, some SSTTs, such as fracture toughness, fatigue, and fatigue crack growth rate, are measured. Because the measurement of the crack growth rate is one of the tests planned for the specimens irradiated at the HFTM, a small-sized specimen for the crack growth has been developed in previous studies [10-11].

Stress corrosion cracking (SCC), i.e., environmentally assisted cracking (EAC), is an important concern in fission reactors. Numerous studies have been performed to examine EAC to understand its mechanisms and thereby enhance the safety of reactors. In the case of fusion reactors, EAC is not expected to be a serious concern because the blanket is designed to be replaced periodically to maintain its performance. Actually, no SCC susceptibility was reported for blankets subjected to high-temperature water (between 240°C and 330°C) containing 10 ppm dissolved oxygen (DO) or for those subjected to 300°C water containing 40 ppb DO [12]. In addition, slow strain rate tensile (SSRT) tests have shown that F82H, T91, and T92 steels do not exhibit SCC susceptibility when exposed to supercritical water [13-16].

However, research on the susceptibility of the blanket to EAC should be required because the blanket materials have been demonstrated to be damaged by heavy irradiation in fusion reactors [12]. For example, transgranular stress corrosion cracking has been reported to occur in irradiated F82H specimens during a SSRT test at 300°C in hydrogenated water or in oxygenated water [17]. Therefore, the objective of this study is to determine the crack growth rate of F82H steel in 288°C water using specimens of approximately standard size.

author's e-mail: ito.yuzuru@jaea.go.jp

Table 1 Chemical composition of F82H-IEA heat (wt.%)

C	Si	Mn	P	S	Cu	Ni	Cr	Mo	V	Nb	B	To.N	Sol.Al	Co	Ti	Ta	W
0.09	0.07	0.1	0.003	0.001	0.01	0.02	7.84	0.003	0.19	0.0002	0.0002	0.007	0.003	0.003	0.004	0.04	1.98

2. Material and Methods

2.1 Material

F82H steel, supplied by the Japan Atomic Energy Agency (JAEA), was used in crack growth tests. The F82H steel was from F82H-IEA heat No. 9753 [18]. The chemical composition of the material is summarized in Table 1. The yield stress of the F82H steel was approximately 607 MPa at room temperature (RT).

2.2 Specimens

For mechanical tests of small specimens, highly accurate control of the applied stress and displacement is required [9]. Therefore, the loading mechanism and/or method for the specimen should be simple and not involve large loading devices for manipulation of the irradiated specimens in the hot cell. Although compact tension (CT) specimens are commonly used in fracture tests, the wedge-opening load (WOL) specimen was used in this study because only the loading bolt and pin are required for the fixturing and only tightening of the loading bolt is necessary to apply a load to the specimen. The tests could be simplified if the WOL specimen was set up with the loading bolt and pin before irradiation because mere tightening of the loading bolt could initiate the crack growth test.

The WOL specimen was designed in accordance with the Standard Test Method for Stress Corrosion Cracking edited by the 129th Committee on Strength and Fracture of Advanced Materials, Society of Materials Science, Japan [19]. Although the standard size of a WOL specimen is regarded as 81.0 mm × 63.0 mm × *t*25.4 mm, fabrication of such standard-sized WOL specimens from the supplied F82H steel was impossible because the size of the as-obtained specimen was limited. However, stress concentration has been reported to strongly affect crack growth in simulated boiling water reactor (BWR) environments [20], and the crack growth rate is known to increase when the plastic area becomes large [21]. Thus, a 0.75T-WOL specimen with

Table 2 The required specimen thickness

Yield Stress [MPa]	607						
K [MPa√m]	15	20	25	30	**30.6**	**48.6**	54
> B [mm]	1.5	2.7	4.2	6.1	**6.35**	**16.0**	20.0

dimensions of 61 mm × 47 mm × *t*16 mm was used in the present work to minimize the effect of the specimen size on crack growth in water at 288°C because the 0.75T-WOL specimen was the largest specimen obtained from the supplied F82H steel. The geometry of the 0.75T-WOL specimen with a thickness of 16 mm is shown in Fig. 1. Given the yield stress of 607 MPa in the F82H steel and the specimen thickness required by ASTM-E399, the stress intensity factor, K, of 48.6 MPa·m$^{1/2}$ was applied to the 0.75T-WOL specimen in this study (Table 2).

The stress intensity factor, K, for the WOL specimen is calculated from the displacement induced at the mouth of the crack by tightening the loading bolt, as monitored by the crack-opening displacement (COD) gauge, and from the crack length at that moment. The displacement at the mouth of the crack required to apply the stress intensity factor K_0 with crack length a_0 is calculated by equation (1) [19].

$$V_0 = \left[\frac{K_0}{E}\right]\sqrt{a_0}\left[\frac{C_6(a_0/W)}{C_3(a_0/W)}\right] \quad (1)$$

where V_0 is the displacement at the mouth of the crack, which is identical to the COD, W is the width of the specimen, K_0 is the stress intensity factor, E is the elastic modulus, a_0 is the crack length, and C_6 (a_0/W) and C_3 (a_0/W) are coefficients. The coefficients C_6 (a_0/W) and C_3 (a_0/W) are calculated from equations (2) and (3):

$$C_3\left(\frac{a}{W}\right) = 30.96 - 195.8\left(\frac{a}{W}\right) + 730.6\left(\frac{a}{W}\right)^2 - 1186.3\left(\frac{a}{W}\right)^3 + 754.6\left(\frac{a}{W}\right)^4 \quad (2)$$

$$C_6\left(\frac{a}{W}\right) = \exp\left[4.495 - 16.130\left(\frac{a}{W}\right) + 63.838\left(\frac{a}{W}\right)^2 - 89.125\left(\frac{a}{W}\right)^3 + 46.815\left(\frac{a}{W}\right)^4\right] \quad (3)$$

For the WOL specimen, we note that K decreases as the

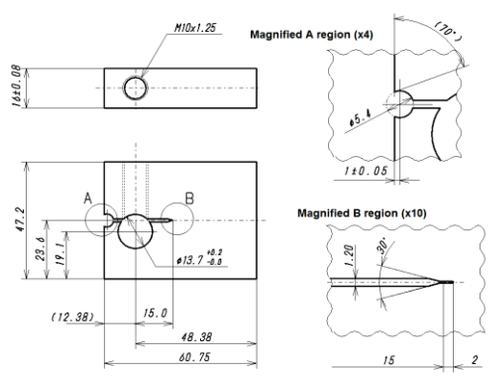

Fig. 1 The 0.75T-WOL specimen with 16 mm-thickness.

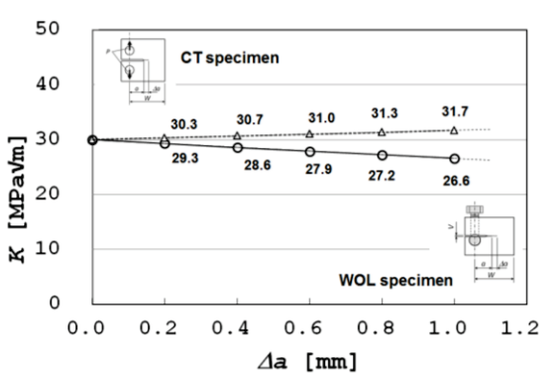

Fig. 2 The variation of K due to the crack propagation in case of WOL specimen and CT specimen.

crack propagates because of the constant COD, as shown in Fig. 2. Reduction of K due to crack propagation is estimated to be approximately 11% for 1.0 mm of crack propagation. In comparison, the variation of K caused by the crack propagation of a CT specimen tested under constant loading mode is also plotted in Fig. 2. In the case of the CT specimen, crack growth rate tests are generally performed under constant loading mode. The value of K increases approximately 6% at 1.0 mm of crack propagation.

2.3 Fatigue pre-cracking in air

After the WOL specimen was fabricated, a fatigue pre-crack of approximately 1.0 mm was introduced at RT in air. Because we intended to conduct the crack growth tests at K = 25 MPa·m$^{1/2}$, the maximum K of the fatigue pre-cracking was 20 MPa·m$^{1/2}$, which is approximately 20% less than that of the crack growth test. The stress intensity factor of the WOL specimen was calculated using the following equation (4) [19]:

$$K = \frac{P\sqrt{a}}{BW}\left[30.96 - 195.8\left(a/W\right) + 730.6\left(a/W\right)^2 - 1186.3\left(a/W\right)^3 + 754.6\left(a/W\right)^4\right] \quad (4)$$

where, P is the applied load, B is the specimen thickness (=16 mm), and W is the specimen width (=48.38 mm).

2.4 Crack growth tests in 288°C water

The crack growth tests in water at 288°C with an electrical conductivity less than 2 × 10^{-4} mS/cm under 2 ppm DO were conducted using an autoclave manufactured by TOSHIN KOGYO CO., LTD. The WOL specimen was placed in the autoclave after the test load was applied at RT in air. Then, the water was heated to 288°C and maintained at this temperature in the autoclave during the test period to immerse the WOL specimen. The test period in this study was approximately 1027 h. The loading procedure is shown in Fig. 3. In this study, a 5% overload, K = 31.5 MPa·m$^{1/2}$, compared to the test load was applied approximately 1 minute at RT in air before the test load was applied, which was expected to promote EAC under the experimental conditions because of further hardening of the plastic zone at the specimen.

Water with 8 ppm DO, where the water is almost saturated with oxygen, is normally regarded as a severe environment for materials. However, higher DO levels do not represent a severe environment for F82H steel, as indicated by previous reports [12] of the general corrosion performance of F82H steel under higher DO levels. Therefore, the crack growth tests were conducted in water containing 2 ppm DO by referring to the water conditions [22] under which crack growth was observed in type 304 stainless steel. Notably, zirconium metal was used to fabricate the loading bolt and pin. After the loading bolt and pin were fabricated, a zirconium oxide film was formed on the fixtures. This film provides an electrically insulating layer between the WOL specimen and the loading bolt and pin, which prevents the formation of a local cell between the WOL specimen and its fixtures in the water.

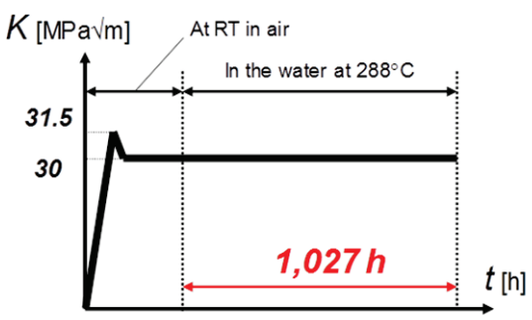

Fig. 3 Loading procedure for 0.75T-WOL specimen.

3. Results and Discussion

3.1 Fracture surface observations

The surface of the specimen was fractured via fatigue post-cracking at RT in air after the crack growth test was terminated. Optical microscopy (OM) and scanning electron microscopy (SEM) were used to observe the fracture surface. The boundary between the pre-cracked area and post-cracked area was sharply defined (Fig. 4). A typical intergranular fracture surface and some oxides were observed, as shown in Fig. 5. Figures 6 (a) and (b) show images of typical intergranular fracture surfaces at the pre-cracked area and the post-cracked area, respectively. Because the pre-cracked area was exposed to 288°C water during the test period, some oxides were observed on the surface. The features of the surfaces observed in Figs. 6 (a) and (b), however, were similar, with the exception of the oxides on the surface in Fig. 6 (a). Therefore, the typical intergranular fracture surface was obtained during the crack propagation at RT in air. Therefore, the area tested for crack growth and the pre-cracked area were difficult to distinguish by merely observing the features of the fracture surface. The possible mechanism of the intergranular fracture of F82H steel at RT in air is discussed in section 3.3.

3.2 Crack growth rate in 288°C water

As previously mentioned, assessing whether the crack growth occurred during the test period only through observation of the features of fracture surface is difficult. Figure 7 shows typical intergranular fracture surfaces following the boundary between the pre-cracked area and post-cracked area. Although the intergranular fracture surfaces are identified in both Figs. 7 (a) and (b), oxides were not always observed on the surfaces, as shown in Fig. 7 (b). Hence we hypothesized that the intergranular fracture surface with some oxides along the boundaries between the pre-cracked and post-cracked areas was evidence of crack growth during the test period, as shown in Fig. 7 (a).

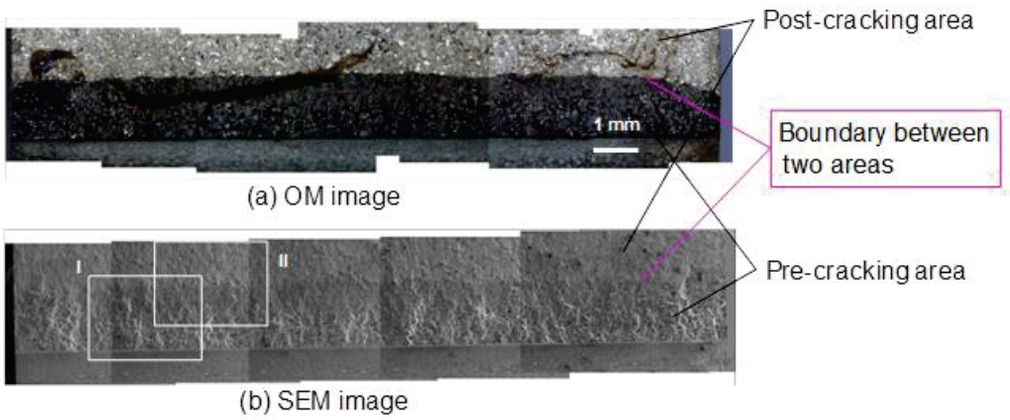

Fig. 4 Fracture surface observed by (a) optical microscope, and (b) scanning electron microscope.

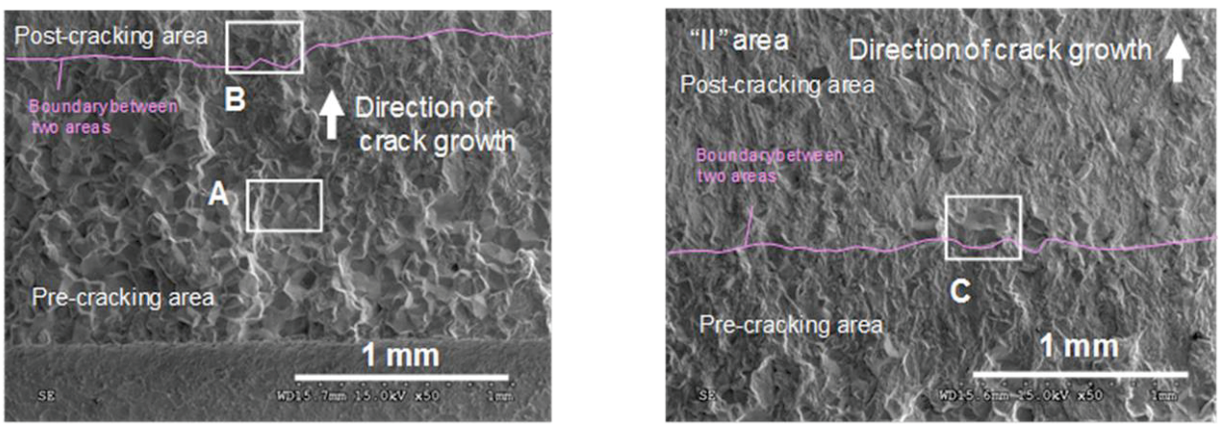

(a) (b)

Fig. 5 Typical intergranular fracture surfaces, (a) "I" zone, and (b) "II" zone.

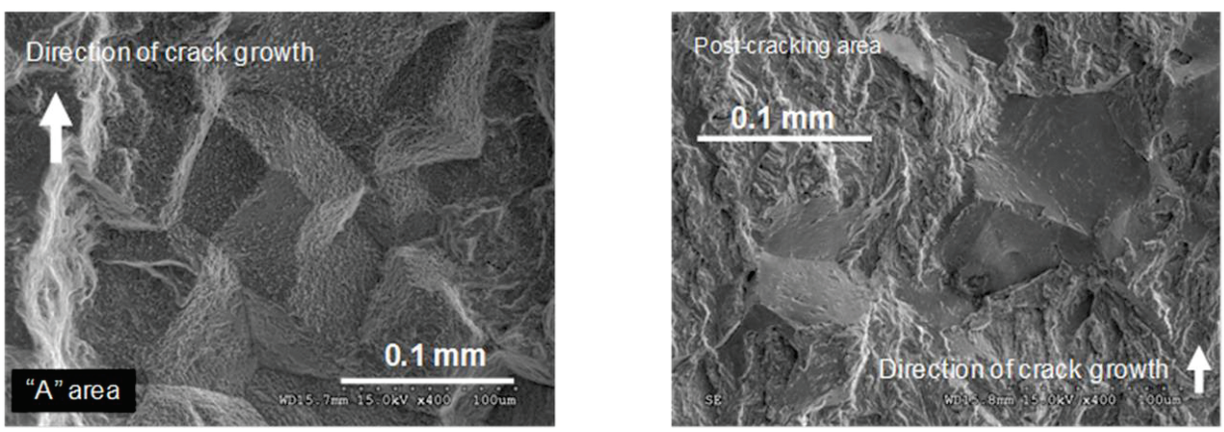

(a) (b)

Fig. 6 Typical intergranular fracture surfaces, (a) with some oxides on the surface at "A" area in "I" zone, (b) without oxides on the surface in the post-cracked area.

In this case, the crack growth rate was estimated from the length of the intergranular fracture surface and the duration of the test period. Because the crack-growth-tested area was difficult to distinguish from the pre-cracked area through mere observation of the fracture surface, a length of 0.26 mm was conservatively regarded as the crack growth distance during the test period of approximately 1000 h, although the crack crossed the boundary (Fig. 8). As a result, the crack growth rate at 30 MPa·m$^{1/2}$ was approximately 7 × 10^{-11} m/s, as calculated on the basis of the crack length, 0.26 mm, divided by the test period, 1027 h. For comparison of the calculated crack growth rate in F82H steel, a crack growth rate of approximately 1 × 10^{-10} m/s at 30 MPa·m$^{1/2}$ has been reported for type-304 stainless steel under BWR environment [23], which is similar to the environment used in this study. However, F82H, T91, and T92 steels have not been reported to exhibit SCC during SSRT tests under supercritical water conditions. Because small-sized specimens for crack growth investigations were developed in previous studies [10-11], further crack growth tests

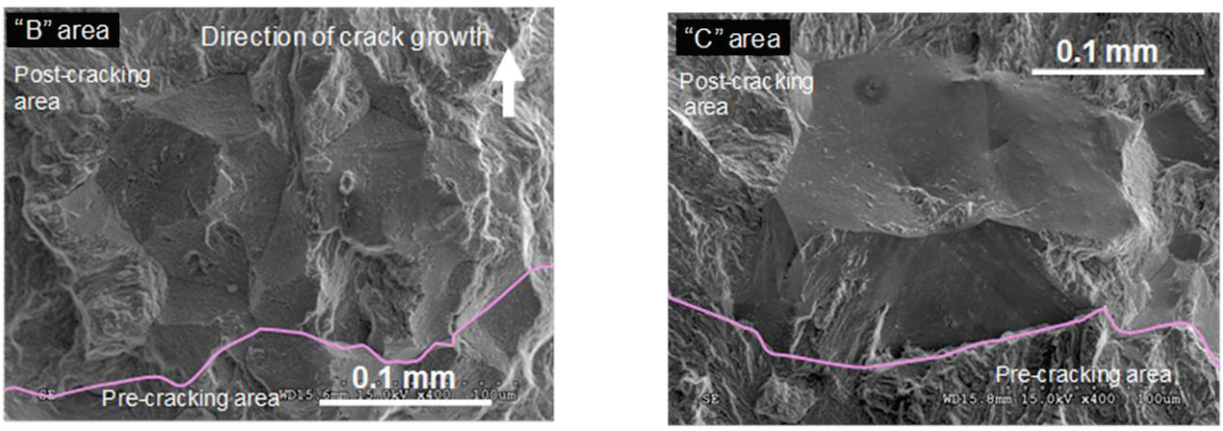

(a) (b)

Fig. 7 Typical intergranular fracture surfaces, (a) with some oxides on the surface at "B" area in "I" zone, (b) without oxides on the surface at "C" area in "II" zone.

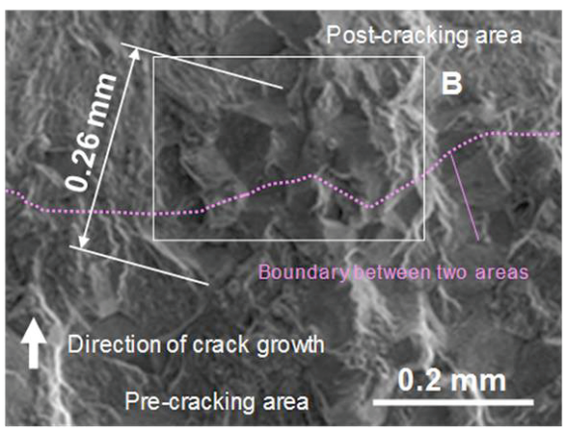

Fig. 8 The measured crack length under the test period, the picture is magnified from Fig. 7 (a).

under high-temperature water conditions, including supercritical water conditions, using the same specimens would be necessary to confirm the crack growth behavior obtained in the 288°C water used in this study.

3.3 Intergranular fracture in F82H steel

We observed that intergranular fracture occurred even in the fatigue pre-crack at RT in air. The fraction of intergranular fracture surfaces at the pre-cracked area in Fig. 5 (a) was measured to be approximately 58%. An intergranular fracture at RT in air has also been reported [24] in thermally treated Alloy 690 (Alloy 690TT). Alloy 690TT [25-27] is a nickel-based, high-chromium, heat-treated alloy; it was developed to improve resistance to intergranular SCC in high-temperature water resulting from the precipitation of chromium carbide, $Cr_{23}C_6$, along the grain boundaries. F82H steel also contains precipitates along the grain boundaries to enhance the resistance to radiation and to maintain toughness under high temperatures. As in the case of Alloy 690TT, the major precipitates in F82H steel are chromium carbide, $Cr_{23}C_6$ [28]. Recently, the $Cr_{23}C_6$ in F82H steel was reported to capture hydrogen isotopes with relatively high stability because the binding energy for hydrogen in $Cr_{23}C_6$ is approximately 0.58 eV [29]. This behavior implies that F82H steel has the potential to trap hydrogen in the material. Therefore, intergranular fracture of F82H steel at RT in air has been attributed to hydrogen embrittlement (HE), where the hydrogen is supplied by the $Cr_{23}C_6$ precipitates [11]; that is, some $Cr_{23}C_6$ in the plastic zone, where cracks are formed, might release captured hydrogen into the grain boundaries and/or into the matrix because of the effect of the stress field of the crack on $Cr_{23}C_6$. The released hydrogen would diffuse along the grain boundary and/or into the matrix; eventually, some hydrogen would concentrate in the high tri-axial stress state region where high stress, high strain, and a high dislocation density coexist. The hydrogen would not only induce HE but also affect the intergranular fracture at RT in air. According to the results of tensile low-strain-rate tests of F82H steel with a 3 wppm hydrogen content, F82H steels exhibit typical brittle fracture consequences of HE; the F82H steels even exhibited HE susceptibility at low hydrogen concentrations of 1–2 wppm [30]. Although $Cr_{23}C_6$ contains less hydrogen initially, the intergranular fracture in F82H steel containing added P has been reported [31] to be induced by grain boundary segregation of P. The grain boundary segregation of P as well as that of $Cr_{23}C_6$ was also identified on the intergranular fracture surface in Alloy690TT [32]. This result supports our explanation of why the intergranular fracture was observed at RT in air in F82H steel as well as in Alloy 690TT.

4. Conclusions

We investigated the crack growth in F82H steel to obtain crack growth data for this steel in water at 288°C. The results obtained in this study are summarized as follows:

1. A typical intergranular fracture surface in the F82H steel was obtained during the crack propagation at RT in air. Therefore, the crack-growth-tested area and the pre-cracked area were difficult to distinguish by mere observation of the features of the fracture surface.
2. The intergranular fracture surface with some oxides

along the boundaries between the pre-cracked and post-cracked areas provides tentative evidence of crack growth during the test period. The crack growth rate at 30 MPa·$m^{1/2}$ was calculated to be approximately 7 × 10^{-11} m/s because the crack length was 0.26 mm during the test period of 1027 h.

3. A possible mechanism of the formation of the intergranular fracture surface in F82H steel in this study was proposed: the precipitation of chromium carbide, $Cr_{23}C_6$, along the grain boundaries in F82H steel may influence the fracture behavior during cases such as fatigue crack propagation at RT in air.
4. Further crack growth tests under high-temperature water conditions, including a supercritical condition, using small-sized specimens would be necessary to confirm the crack growth behavior observed in water at 288°C.

Acknowledgement

This study was performed under the IFMIF/EVEDA project in the Broader Approach (BA) framework.

References

[1] E. Wakai, N. Hashimoto, Y. Miwa, J.P Robertson, R.L Klueh, K. Shiba, S. Jistukawa, *J. Nucl. Mater.* **283-287** (2000), pp. 799–805.

[2] E. Wakai, T. Sawai, K. Furuya, A. Naito, T. Aruga, K. Kikuchi, S. Yamashita, S. Ohnuki, S. Yamamoto, H. Naramoto, S. Jistukawa, *J. Nucl. Mater.* **307-311** (2002), pp. 278–282.

[3] E. Wakai, K. Kikuchi, S. Yamamoto, T. Aruga, M. Ando, H. Tanigawa, T. Taguchi, T. Sawai, K. Oka, S. Ohnuki, *J. Nucl. Mater.* **318** (2003), pp. 267–273.

[4] T. Tanaka, K. Oka, S. Ohnuki, S. Yamashita, T. Suda, S. Watanabe, E. Wakai, *J. Nucl. Mater.* **329-333** (2004), pp. 294–298.

[5] T. Taguchi, N. Igawa, S. Miwa, E. Wakai, S. Jitsukawa, L.L. Snead, A. Hasegawa, *J. Nucl. Mater.* **335** (2004), pp. 508–514.

[6] E. Wakai, M. Ando, T. Sawai, K. Kikuchi, K. Furuya, M. Sato, K. Oka, S. Ohnuki, H. Tomita, T. Tomita, Y. Kato, F. Takada, *J. Nucl. Mater.* **356** (2006), pp. 95–104.

[7] IFMIF Comprehensive Design Report, by the international Team, an Activity of the international Energy Agency, Implementing Agreement for a program of Research and Development on Fusion Materials, January 2004.

[8] A. Möslang, "Development of a Reference Test Matrix for IFMIF Test Modules", *Final Report on the EFDA Task TW4-TTMI-003 D4*, 2006.

[9] E. Wakai, M. Yamamto, J. Molla, T. Yokomine, S. Nogami, *Fus. Eng. Des.* **86** (2011), pp. 712–715.

[10] Y. Ito, M. Saito, K. Abe, M. Yamamoto, E. Wakai, *ICFRM16*, Paper ID. 16–477, Beijing, China, Oct. 20–26, 2013.

[11] Y. Ito, M. Saito, K. Abe, E. Wakai, *ASTM 6th Int. Symp. on Small Specimen Test Techniques*, Houston, TX, Jan. 29–31, 2014.

[12] Y. Miwa, T. Tsukada and S. Jitsukawa, *J. Plasma Fus. Res.* **80**, No.7 (2004), pp. 551–557.

[13] T. Hirose, K. Shiba, M. Enoeda, M. Akiba, *J. Nucl. Mater.* **367–370** (2007), pp. 1185–1189.

[14] G. Gupta, G. S. Was, *Proc. 12th Int. Conf. on Environmental Degradation of Materials in Nuclear Power Systems –Water Reactors, The Minerals, Metals and Materials Society*, pp. 1359–1367, Snowbird, UT, Aug. 15–18, 2005.

[15] P. Ampornrat, C. B. Bahn, G. S. Was, *Proc. of the 12th Int. Conf. on Environmental Degradation of Materials in Nuclear Power Systems –Water Reactors, The Minerals, Metals and Materials Society*, pp. 1387–1396, Snowbird, UT, Aug. 15–18, 2005.

[16] S. S. Hwang, B. H. Lee, J. G. Kim, J. Jang, *J. Nucl. Mater.* **372** (2008), pp. 177–181.

[17] Y. Miwa, S. Jitsukawa, T. Tsukada, *J. Nucl. Mater.* **386–388** (2009), pp. 703–707.

[18] K. Shiba, A. Hishinuma, A. Tohyama and K. Kasamura, *JAERI-Tech 97-038*, JAERI, 1997.

[19] Society of Materials Science, Japan, Standard Test Method for Stress Corrosion Cracking, 129th Committee on Strength and Fracture of Advanced Materials (1985), pp. 8–17.

[20] T. Sato and T. Shoji, Effects of Specimen Size and Thickness on CGR in High Temperature Waters, *Proc. 11th Int. Conf. Environmental Degradation of Materials in Nuclear Systems*, pp. 862–869, Stevenson, WA, Aug. 10–14, 2003.

[21] T. Shoji, S. Suzuki, R. G. Ballinger, Theoretical Prediction of SCC Growth Behavior Threshold and Plateau Growth Rate, *Proc. 7th Int. Symp. on Environmental Degradation of Materials in Nuclear Power Systems-Water Reactors*, pp. 881–892, Houston, TX, Aug. 7–10, 1995.

[22] Y. Ito and M. Saito, *16PBNC*, Paper ID. P16P1164, Aomori, Japan, Oct. 13–18, 2008.

[23] S. Namatame, S. Suzuki, N. Tanaka, M. Itow, J. Kuniya, S. Shimanuki, *JSME annual meeting 2002(1)*, pp. 441–442.

[24] Y. Ito, Z. P. Lu, H. Miura, T. Yonezawa, T. Shoji, *JSME Int. J. Series A* **49**, No.3 (2006), pp. 355–362.

[25] T. Kusakabe, T. Yonezawa, S. Tokunaga, *Mitsubishi Heavy Industries Technical Review* **32**, No.3 (1995), pp. 161–164.

[26] M. Thuvander, K. Stiller, *Mater. Sci. Eng. A* **281**, No.1–2 (2000), pp. 96–103.

[27] T. Yonezawa, *Met. Technol. (Jpn.)* **73**, No.8 (2003), pp. 727–730.

[28] H. Tanigawa, H. Sakasegawa, K. Shiba and T. Hirose, *J. Plasma Fus. Res.* **87**, No.3 (2011), pp. 167–171.

[29] Y. Watanabe, H. Iwakiri, N. Murayoshi, D. Kato, *29th JSPF Annual Meeting*, ID.05aD04P, Tokyo, Japan, Dec. 3–6, 2013.

[30] M. Beghini, G. Benamati, L. Bertini, R. Valentini, *J. Nucl. Mater.* **258–263** (1998), pp. 1295–1299.

[31] B.J. Kim, R. Kasada, A. Kimura, H. Tanigawa, *J. Nucl. Mater.* **421** (2012), pp. 153–159.

[32] Y. Ito, Z.P. Lu, H. Miura, T. Shoji, *Proc. 52nd Japan Conf. on Materials and Environments*, pp. 231–234, Sapporo, Japan, Sep. 14–16, 2005.